Strål säkerhets myndigheten
Swedish Radiation Safety Authority

Author: Torbjörn Bäck,
Royal Institute of
Technology, Stockholm

Research

2018:13

Prestudy: Detectors for variance measurements in the nanometer range

Report number: 2018:13 ISSN: 2000-0456
Available at www.stralsakerhetsmyndigheten.se

SSM perspective

Background

The understanding of radiation quality requires knowledge about the energy deposition pattern of ionizing radiation on which models for cellular and sub-cellular damage can be built. Experimental data is fundamental in this context for quality assurance and bench-marking of models and simulations. Direct measurements are also of practical importance for radiation quality determinations in radiation therapy and radiation protection.

In the experimental microdosimetric variance-covariance method, the radiation quality is determined from the dose average lineal energy (y_D) that is used as an approximation of the dose average linear energy (LET_D). The method has been successfully used in several radiation protection applications and the importance of the dose average lineal energy determined at 10 nm object sizes has also shown to be of potential importance for radiation quality measurements in radiation therapy. There is however a need for detector and method development to obtain robust dose average lineal energy measurements with sufficiently low uncertainties at 10 nm or smaller object sizes.

Objective

The objectives of this project were to give an overview of existing micro- and nanodosimetric detectors and measurement techniques, identify a few potentially promising detector types and geometries for measurement of the dose-average lineal energy for 10 nm objects using the variance-covariance method, summarize simulation needs for the development of a suitable detector design, and to outline a suitable strategy for detector and method development for improvement of experimental nanodosimetry using the variance-covariance method

Results

Conventional ion chambers with low-noise electrometers has been used for nanodosimetry with the variance-covariance method down to the 10 – 50 nm range. It is concluded that this is also a potentially promising approach even for smaller object sizes. A better understanding of the influence from secondary electrons and anode, together with an improved electrometer design are though needed. Some additional development needs for detectors and simulations, as well as potential novel detector solutions for the variance-covariance method are briefly outlined.

Need for further research

Aspects to investigate further for ion chamber based variance-covariance measurements are the influence of electronic noise, anode geometry and secondary electron emission. This should be addressed by improved electronics and measurements with, and simulations of different ionization chamber designs and sizes. Various existing conventional

ion chambers should be used with existing electrometers, and compared with modern commercial electrometers to validate previously obtained results. The potential of using larger detectors for reaching smaller object sizes should also be investigated.

A novel technique of interest for nanodosimetric research in general could be using a multi-channel-plate for ionization track characterization and nanodosimetric analyses. It is also pointed out that the use of parallel-plate gas detectors with the variance-covariance method for this purpose has not been fully explored and could be of potential further interest. In addition the formalism relating the dose-average lineal energy to ion cluster formalism should be developed. Finally a simulation tool using coupled simulations of radiation interaction and detection processes would be of great importance for the development of new detector and electrometer designs.

Project information
Contact person SSM: Jan Lillhök
Reference: SSM2015-2092

Strål
säkerhets
myndigheten
Swedish Radiation Safety Authority

Author: Torbjörn Bäck,
Royal Institute of
Technology, Stockholm

2018:13

Prestudy: Detectors for variance measurements in the nanometer range

Date: January 2018
Report number: 2018:13 **ISSN:** 2000-0456
Available at www.stralsakerhetsmyndigheten.se

This report concerns a study which has been conducted for the Swedish Radiation Safety Authority, SSM. The conclusions and viewpoints presented in the report are those of the author/authors and do not necessarily coincide with those of the SSM.

Prestudy: Detectors for variance measurements in the nanometer range

Torbjörn Bäck, Royal Institute of Technology, 2016

Contents

1 Introduction

The understanding of how ionization radiation of a certain type, energy-, and intensity profile, affects biological tissue has been a central objective in the scientific field of dosimetry and radiobiology over more than a century. Since long it is understood that the basic (sometimes called *macroscopic*) dosimetric quantities, e.g. *absorbed dose* or *dose equivalent*, while useful, are limited in predicting radiobiological effects. These quantities do not consider the spatial *distribution* of the energy as the radiation quanta interacts with the biological tissue. Since we know that the sensitivity of biological tissue is quite unevenly distributed in space and quickly varies between microscopic sub-volumes (e.g. in the vicinity of the DNA molecules in the cell nuclei) it is important to understand how energy deposits - that induce ionization, excitation and structural damage on the atomic scale - are distributed at very small scale (μm, nm) in order to deepen the understanding of the dose-effect relationship. Pioneering work in this direction was done first by Lea [1] and by Rossi and coworkers in the 1950:s and 1960:s, see e.g. Refs. [2, 3, 4, 5], thereby giving the foundation for the discipline that we today call *microdosimetry*. This broad field of research focuses on the stochastic nature of energy deposition from radiation interaction in small volumes of matter.

A detailed knowledge about ionization distributions and particle track structures at the micro/nanometer scale is the key to understanding how structural damage at the cellular and sub-cellular levels develops and how the generation of various free radical molecules are created when radiation interacts with biological tissue. The developments in computer technology in the last few decades and modern Monte Carlo simulation techniques enable us to model the interaction between radiation and matter on the scales of interest here. However, it is of fundamental interest to benchmark theoretical models and simulation results with experimental data. For this the established but still developing field of microdosimetry and the new and upcoming field of nanodosimetry will continue to play a crucial role. At the same time, microdosimetry is already a mature scientific discipline with several applications in various fields, both in determination of the radiation quality in low-dose applications such as radiation protection and in high-dose applications such as radiation therapy.

Measurements using microdosimetric techniques have a long tradition in Sweden and are today well established at the Swedish Radiation Safety Authority (SSM), both for low-LET and high-LET radiation qualities. Of particular success has been the so-called *variance-covariance method*, applied and described in detail in Ref. [6]. This method is in some cases the only choice, i.e. at very high rates and/or at gas pressure below the gas multiplication region. In such cases, the more common *single event method* could be impossible to use, e.g. due to noise limits or problems with event pulse pile-up.

This prestudy was performed during 2015/2016 at KTH in close collaboration with SSM. In the original project proposal an important objective was to investigate how future measurements performed at SSM could be developed into approaching the 10 nm scale, i.e. which detector types that could be suitable for simulating nano-metric volumes with a size in the order of 10 nm or less. Measurements in both low-LET

and high-LET radiation fields were of interest. In particlular the potential use of the variance-covariance method was of high interest. Neither detailed detector designs nor any prototype construction or measurements are part of this prestudy.

An important motive behind addressing the nanometer region with novel experimental techniques is the evidence that the distributions of energies and ionization cluster sizes at the nanometer range seem to correlate well with relevant biological damage. An example of such evidence was given by Brenner and Ward [7] who correlated double strand breaks in the DNA molecule with a small number of ionizations in sites approximately 1-4 nm across.

This prestudy first gives a brief overview of some of the fundamental quantities in microdosimetry and discusses some issues related to their definitions. Then a more recently established alternative formalism based on ionization cluster size, suitable for the nanometer region, is presented. This formalism is especially relevant for applications in hadron therapy where the primary beam follows approximately a linear track, and were the impact parameter of the primary beam can be controlled. The next chapter presents various detector solutions for micro- and nanodosimetry, with a focus on a few novel detector setups for nanodosimetry research. The last chapter discusses suggestions of new detector equipment at SSM with the aim of measuring in sites of sizes at and below 10 nm, and in the longer term approach particle-track imaging on the nanometer scale.

2 Micro- and nanodosimetry – fundamentals

It is not the purpose of this report to give any kind of overview of the fields of micro- and nanodosimetry. However, some of the fundamental quantities and their definitions are discussed below to place the report in a framework of formalism, especially for the non-specialist reader. More importantly, since part of the intent is to discuss aspects of new developments and new possibilities for detector applications at the nano-scale, it is relevant to re-investigate some of the basic quantities related to energy deposits and ionizations. One consequence of the limitations of the traditional formalism is the relatively new formalism of cluster-size formation probabilities, see Section 2.5.

2.1 Basic quantities in microdosimetry

An incoming ionizing particle (e.g. a high energy electron, photon, proton, neutron, heavy ion, ...) will interact with a material by sharing its kinetic energy to the particles of the material. Several different physical processes can be responsible for the energy transfer itself. The material can be e.g. water, human tissue, air, or the gas in a radiation detector. Assuming that this energy transfer takes place only at discrete interaction points, we can, following the definition in Ref. [8], define the *energy deposit*, $\epsilon_{\rm i}$, in a single interaction, i, as:

$$\epsilon_{\rm i} = T_{\rm in} - T_{\rm out} + Q_{\Delta{\rm m}}. \tag{2.1}$$

Here, $T_{\rm in}$ is the kinetic energy of an ionizing incoming particle, $T_{\rm out}$ is the sum of kinetic energies of all outgoing ionizing particles, and $Q_{\Delta{\rm m}}$ corresponds to the sum off all rest mass differences in the system. This definition is however not without problems, for a few reasons. First, we note that $T_{\rm in}$ and $T_{\rm out}$ includes energies only of *ionizing particles*. It is mentioned in a footnote in Ref. [8] that the *energy cutoff*, below which particles are considered to be non-ionizing, will depend on the circumstances. Second, if in the determination of $Q_{\Delta{\rm m}}$ we consider all particles involved, its value should not only depend on high-energy nuclear and particle reactions but also include the difference in mass due to the binding energy difference of an atom that becomes ionized or excited at the interaction point. But that would give $\epsilon_{\rm i} = 0$ also for such cases, and it is rather obvious that that was not the intent of the definition.

Another issue to consider is that the deposited energy as such might not be the only relevant quantity connected to radiation damage of biological tissue. Energy can be absorbed by microscopic structures in different ways, e.g. as heat, not necessary inducing ionization or structural damage. A related problem is that the deposited energy can be very difficult to measure. Normally we measure something else, such as the amount of ionization events. The total imparted energy in a small volume is typically associated with the amount of ionization in a small volume, but the relationship between these quantities is not always easy to evaluate.

If only a small number (say <10) of initial ionization events take place in a small volume of interest, the energy deposit cannot be deduced by using an *average* energy-per-ionization parameter without introducing a large error in the deduced energy. This error will remain independently of any multiplication of charge carriers in the detector.

These issues with the definition of $\epsilon_{\rm i}$ are of course well known in the scientific community. In Refs. [9, 10] (the authors of which must be considered authorities in the field of microdosimetry) some of these problems are discussed in some detail. It seems, perhaps not surprisingly, that the standard interpretation is that by definition $Q_{\Delta{\rm m}} = 0$ for typical atomic excitations/ionizations and $Q_{\Delta{\rm m}} \neq 0$ only in the case of high energy reactions involving nuclear reactions, pair production, etc [9].

In spite of all these difficulties it is clear that the definition of energy imparted and the quantities that follows from it has proven to be very useful, see e.g. Refs. [8, 9, 10] for an overview.

Continuing from Eq. 2.1, still following Ref. [8], we define a number of other quantities established in microdosimetry. If a well defined volume of material is affected by a passing projectile we can sum over all single interactions and define the *energy imparted*, ϵ. We then have $\epsilon = \Sigma_{\rm i}\epsilon_{\rm i}$. It is important here to note that both ϵ and $\epsilon_{\rm i}$ are *stochastic* quantities. This fact in itself will have consequences for the limitations at the nanometer scale, as discussed in section 2.4.

Another stochastic quantity is the *specific energy*, z, defined as:

$$z = \frac{\epsilon}{m}, \tag{2.2}$$

where m is the mass of the volume of interest. Due to the stochastic nature of z it is useful to consider the distribution function, $F(z)$, i.e. the probability that the specific energy is less than or equal to z. Now we can define the probability density, $f(z)$, as:

$$f(z) = \frac{{\rm d}F(z)}{dz}. \tag{2.3}$$

The expectation value of z is a non-stochastic quantity called the *mean specific energy*, $\bar{z}$, and is defined as:

$$\bar{z} = \int_0^\infty z f(z) dz. \tag{2.4}$$

We also define the *lineal energy*, y, the ratio between the energy imparted and the *mean chord length*, $\bar{l}$, for the volume of interest:

$$y = \frac{\epsilon}{\bar{l}}. \tag{2.5}$$

We note here that y is a stochastic quantity. The *chord length*, l, i.e. the length of the path over which the primary radiation particle pass through the volume of interest, is also a stochastic quantity. Usually, l is not measured during an experiment, although it can be done, see section 3.3 below. It can be proven that the non-stochastic quantity $\bar{l}$, is equal to $4V/a$ for a convex body of volume V and surface area, a. For a spherical volume of radius r this means that the mean coord length is equal to $4r/3$.

The lineal energy, y, is related to another quantity, *linear energy transfer (LET)*. Both quantities have the same dimension (energy per length) and both are relevant for the classification of radiation quality. The complex relationship between y and LET is discussed in Ref. [11]. The values of y and LET will not typically be the same at small object sizes. Unlike LET, the lineal energy is defined to be measured.

In the same way as for z, we can define for y the distribution function $F(y)$ and its derivative, called the *lineal energy distribution*, $f(y)$:

$$f(y) = \frac{\mathrm{d}F(y)}{dy}. \tag{2.6}$$

Dose and dose distributions can be defined both for z and y. For example we have $D(y)$, i.e. the fraction of absorbed dose delivered with lineal energy less than or equal to y. The dose probability $d(y)$ is the derivative of $D(y)$ with respect to y:

$$d(y) = \frac{\mathrm{d}D(y)}{dy}. \tag{2.7}$$

The expectation value of $d(y)$ is denoted $\bar{y}_D$, the *dose mean lineal energy*, and is defined as:

$$\bar{y}_D = \int_0^\infty y d(y) dy. \tag{2.8}$$

The lineal energy, y, and the dose distribution $d(y)$ contains valuable information about the radiation modality and energy. As an example, we could consider a plot of $yd(y)$ vs y for different types of radiation in the same small simulated volume. Each curve will reflect the distribution of deposited energies, expressed as lineal energies in the volume. As an example, compared to a low-LET radiation (e.g. gamma photons near 1 MeV from a Co-60 source) a beam of high-LET radiation, such as 3.7 MeV neutrons, will have a distribution shifted towards higher y-values, as illustrated in the schematic plot below.

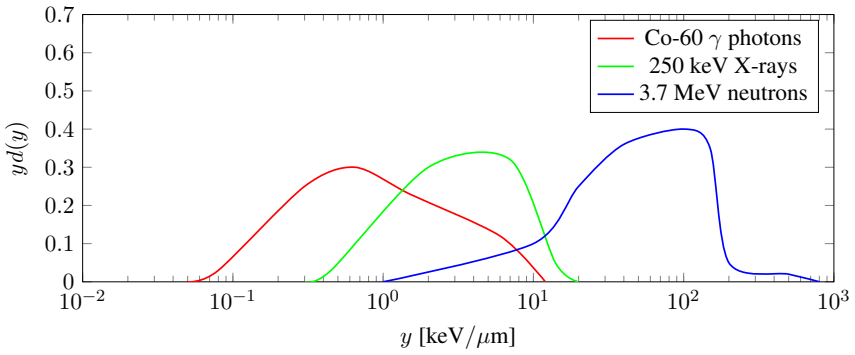

Figure 2.1: Schematic picture (not measurement data) to illustrate how the lineal energy distribution depends on radiation quality. The plot corresponds roughly to measurements in spherical tissue regions of 1 μm size, see e.g. Ref. [8].

The most common way to deduce experimental data, like e.g. the $yd(y)$ vs y-plots, is to collect single-event pulses, each pulse generated by a primary particle passing the sensitive detector volume and interacting with the gas atoms to generate a number of ion-electron pairs. The free electrons would then typically be accelerated (and, providing the pressure is high enough, be multiplied) in the electric field of the detector and generate a single charge pulse that could be amplified and collected by the acquisition system. If the number of electron-ion pairs generated by the primary particle is large, the amplitude of this charge pulse is approximately proportional to the energy imparted, ε, of the event and therefore this amplitude can give a measure of the lineal energy, y. A large number of events will together be used to get the full $yd(y)$ vs y spectrum.

2.1.1 Lineal energy and relative biological effectiveness

The quantity $\bar{y}_d$ has a bearing on the relative biological effectiveness (RBE). The relationship between $\bar{y}_d$ and so-called *weighting factors*, formally *quality factors*, is a long-standing question in the field of dosimetry, and important for regulatory agencies such as ICRP and SSM. Different models have been proposed over the years, and although it is generally agreed that RBE is related to $\bar{y}_d$ at small object sizes, there is no final consensus on a model at the present time. A commonly used model based on clinical therapy experience is the linear-quadratic (LQ) relationship for the biological effect (BE) as a function of the absorbed dose, D:

$$BE = \alpha n d + \beta n d^2 \tag{2.9}$$

$$BE = \alpha D \left(1 + \frac{d}{\alpha/\beta}\right), \tag{2.10}$$

where D is distributed in the tissue in n equal fractions, each with dose d. If one accepts this model, the remaining work is then to determine α and β for the various radiation qualities. An up-to-date discussion on how measured $\bar{y}_d$ ratios between two radiation qualities relate to the corresponding α ratios is given in Refs. [12, 13] in the specific context of radiation therapy. From this work there is evidence that $\bar{y}_d$ values measured in the 10-15 nm range are particular relevant in that the $\bar{y}_d$ ratios seem to become proportional to the α ratios, independent on radiation quality [12, 13].

2.2 The variance method

The quantity $\bar{y}_D$ in Eq. 2.8 is usually called the *dose mean lineal energy*. It can easily be extracted from the lineal energy distribution in a single-event measurement, corresponding e.g. such spectra as in Fig. 2.1.

There is however a method to measure the $\bar{y}_D$ quantity directly without producing a single-event spectrum first. This method utilizes the statistical fluctuations in energy imparted, ε, in the measurement. Several parameters in a specific measurement can contribute to these fluctuations. The statistical distribution of the number of ionization points in the detector gas value is especially important at low gas pressures (small simulated volumes). Electronic noise, the distribution of chord-length, and variations in the radiation flux, are other parameters contributing to the fluctuations in ε.

We now denote the frequency mean value of ε as $\bar{\varepsilon}$ and the total relative variance in a multiple-event spectrum as V_r. The dose, D, and the dose mean lineal energy, $\bar{y_D}$, in a detector volume with mass m, can be expressed as:

$$D = \frac{\bar{\varepsilon}}{m} \tag{2.11}$$

and

$$\bar{y}_D = \frac{V_r \bar{\varepsilon}}{\bar{l}}. \tag{2.12}$$

By measuring the fluctuating detector current as a function of time in a constant radiation field, a value for $\bar{y}_D$ can thus be determined without the need to produce e.g. the $yd(y)$ vs y spectrum. This so-called *variance* method was pioneered by Bengtson and Lindborg in the 1970s [14, 15].

Compared to the single-event pulse method the variance method has an obvious disadvantage in that it gives less detailed information about the radiation quality. This method can for example not produce spectra like those in Fig. 2.1, and it might not be the best tool of choice when the radiation quality is unknown or when we have a mix between two or more radiation qualities. The variance method does however carry important advantages. Single pulse-event based acquisition systems have limitations at count rates due to pile-up of sequential individual pulses. Since applications are not limited to cases when the charge pulses from the detector can be separated from each other, the variance method is convenient to use in high-flux applications. If, for example, the radiation field is generated by a pulsed accelerator, a single accelerator pulse could generate a large number of charge pulses in the detector in a very short time interval. Another important advantage comes from the fact that a continuous charge current can be measured even without charge-multiplication in the detector volume. Therefore the variance method works for tissue-equivalent ionization chambers at very low gas pressures. This feature makes it suitable for performing measurements at simulated sizes in the nanometer range.

2.3 The variance-covariance method

The basic variance method measurements relies on the assumption of having a *constant* radiation flux. The charge integration is typically performed over fixed time intervals and the signal then corresponds to an approximately equal dose per interval. The method fails if the radiation flux is considerably changing over time. The reason is that the parameter V_r will depend both on the particle-event-by-event variance of ε and on the changing radiation flux.

A development in the methodology was made by Kellerer and Rossi in 1984 by introducing a second detector operating in parallel and by including the covariance between the two detector signals in the formalism [16]. Here it is important that the second detector is designed and positioned in such a way so that the events in the two detectors are uncorrelated; a primary particle in one of the two detectors should i.e. not generate a signal (direct or indirectly) in the other detector. The two detectors do however not have to be identical, or even placed in the same radiation field intensity. It is however a requirement that the dose rates measured in the two detectors should be proportional to each other. If we consider a setup with two detectors, A and B, the expression for the dose mean lineal energy measured by detector A can be written:

$$\bar{y}_D = (V_r - C_r)\frac{\bar{\varepsilon}}{\bar{l}}, \tag{2.13}$$

where C_r is the relative covariance of the signals of the two detectors. Alternatively, as in Ref. [6], $\bar{y}_D$ can be expressed in terms of the mean specific energies, $\bar{z}$, measured in detectors A and B:

$$\bar{y}_D = \frac{m}{\bar{l}}(V_r - C_r)\bar{z}_A = \frac{m}{\bar{l}}\left[\frac{\overline{z_A^2}}{\bar{z}_A} - \frac{\overline{z_A z_B}}{\bar{z}_B}\right]. \tag{2.14}$$

Further developments has been made in the formalism and in the methodology in variance measurements. More detailed information can be found in Ref. [6].

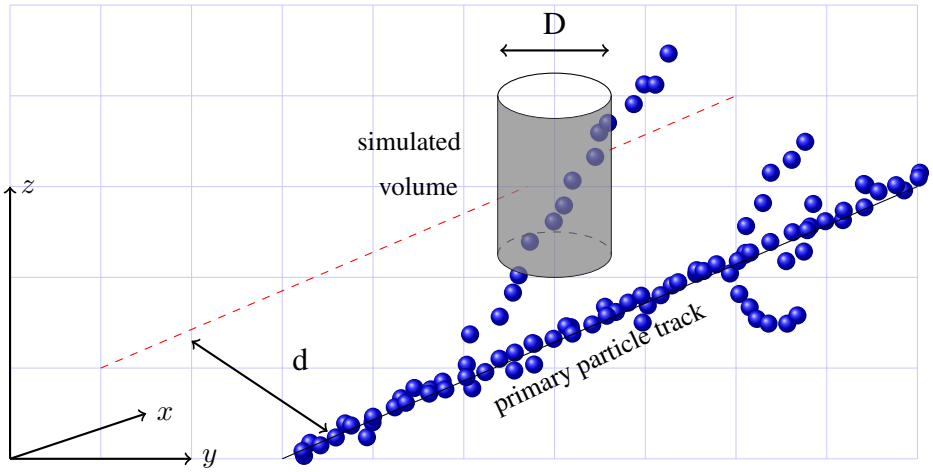

Figure 2.2: An illustration relevant for the ionization probability formalism in nano-dosimetry. For a specific radiation quality, Q, and for each distance, d, between the primary particle track and the centre of the sensitive volume, there will be a probability, $P_\nu(Q;d)$, that exactly ν ions are detected in the sensitive volume.

2.4 Limits at the nanometer scale

At volume sizes in the order of 10 nm and smaller, the formalism presented so far has limitations. Since the quantity measured in a typical gas-filled micro-dosimetric detector (e.g. a TEPC) in reality is not the energy imparted, ε, but rather the number of electron-ion pairs created in the sensitive volume of the detector, a parameter, W, is used to provide the ratio between number of ion-e$^-$ pairs and ε for each event. When each detector event corresponds to a large number of ionizations it is reasonable to use such a constant W-value, but at the nano-scale where the number of ionizations is often a small number, the method fails.

The non-trivial relationship between loss by total deposited energy and ionization loss in volumes of sizes ranging from 1 nm to 1 μm was investigated by Amols et. al [17]. They used Monte Carlo simulations for the comparison and confirmed that the lineal energy originating from ionization loss differ dramatically from total deposited energy below 10 nm, in particular in the low-energy range of the spectrum. Such simulations are useful when interpreting data at the nanometer scale i.e. by determining suitable correction factors.

The problem of choosing the most relevant quantity from a measurement is however nontrivial, since biological effects are likely to depend in a different way on ionization, compared to deposited energy.

2.5 Cluster-size formation probabilities

An alternative to the above formalism based on energy deposits along the particle track is to consider the distribution of *ionization clusters* in nanometer-scale sub-volumes. This is one way to avoid some of the problems mentioned above, especially the stochastic nature of the number of ionization events per deposited energy. Another thing to

consider is that the penumbra of secondary electrons surrounding a particle track is small compared to the simulated volume at the μm scale, but not at the nano scale. The geometric relationship between the primary particle vector and the simulated volume is therefore important for objects of nanometer size. One way to address this is to include a parameter such as the *impact parameter* in the formalism. We can, see Fig. 2.2 and following e.g. Refs.[18, 19], consider a single primary particle of radiation quality, Q, following a track passing a well-defined sub-volume at closest distance, d. The number of ionizations formed inside the sub-volume produced by the single passing primary particle (including secondary electrons) is now a relevant observable. The probability that this number of ionizations is exactly equal to the integer ν is now denoted as:

$$P_\nu(Q;d). \tag{2.15}$$

From this definition of P_ν we immediately get

$$\sum_{\nu=0}^{\infty} P_\nu(Q;d) = 1. \tag{2.16}$$

The statistical moments of P_ν, of k:th order, is denoted $M_k(Q;d)$ and can be expressed as:

$$M_k(Q;d) = \sum_{\nu=0}^{\infty} \nu^k P_\nu(Q;d). \tag{2.17}$$

The mean ionization cluster size corresponds to the first moment, M_1, of P_ν:

$$M_1(Q;d) = \sum_{\nu=0}^{\infty} \nu P_\nu(Q;d). \tag{2.18}$$

The cumulative probability distribution, F_k, i.e. the probability that an ionization cluster size of k *or larger* is created in the volume of interest is expressed as:

$$F_k(Q;d) = \sum_{\nu=0}^{\infty} P_\nu(Q;d). \tag{2.19}$$

It can be argued, see e.g. Ref. [20], that some of the above quantities would behave similar to the probability for radiation damage of the DNA molecule in biological tissue. In a volume of DNA-molecule size (i.e. at nanometer scale), for a certain radiation quality, one could e.g. expect that single strand breaks in DNA would behave like the quantity P_1, i.e. the probability that $\nu = 1$, and that double-strand breaks would behave like F_2, i.e the cumulative probability that $\nu \geq 2$. Other quantities can also be expressed in P_ν and its moments, such as the *variance* of the cluster size formation, σ_ν^2:

$$\sigma_\nu^2 = \sum_{\nu=0}^{\infty} \nu P_\nu(Q;d) - \sum_{\nu=0}^{\infty} \nu^2 P_\nu(Q;d). \tag{2.20}$$

One could argue that this formalism is more relevant or suitable in cases where the number of ionizations (in the volume of interest) per incoming primary particle is a small number. It is also particular relevant for those cases when a primary particle follows, approximately, a linear path, while generating clusters of secondary electrons surrounding this path. This is the case for high-energy proton beams (and also heavy-ion beams) used for radiotherapy, an application of high interest today. In nanodosimetry research

the parameter d is often controlled in the experimental setup. This can for example be achieved by sweeping a collimated proton beam in a controlled way near or inside the sensitive volume, and/or by detecting the primary particle in a separate position-sensitive detector downstream from the sensitive volume.

When a series of measurements for several values of the distance d is performed, it should be a straight forward procedure to deduce the ionization distribution (in number and space) in several different beam profiles and also to deduce microdosimetric quantities such as lineal energy distributions by integrating over the detector cross section. This could potentially be a way to benchmark nanodosimetric measurements to e.g. gas detector measurements using the variance-covariance method when approaching the nano-scale. The expressions in equations 2.18 and 2.20 above could be useful in such comparisons. However, it seems that the variance-covariance method has typically not been used in setups where the impact parameter, d, was controlled. If such a measurement was performed, experimental results at the nano-scale such as those presented in e.g. Ref.[21] could be independently tested by the variance-covariance method.

For detector-design purposes, e.g. for measurements using the variance-covariance method, it is valuable to be able to estimate the mean values and variances of ionization cluster-size distributions. To get an idea about the approximate cluster size distributions we can start by looking at the simple case of $d = 0$, so that the primary particle beam passes through the centre of the sensitive volume. Since the majority of ionizations in this case will be due to the primary particle ionization track, we can attempt to make a Poisson distribution approximation for $P_\nu(Q; d = 0)$. The result, see Fig. 2.3, shows the dependence of gas pressure on the cluster size formation distributions. The mean value at $D\rho = 0.2$ is normalized to the value in Fig.2 of Ref. [19], and it is assumed that the mean number of primary ionization is proportional to the mass density. In spite of the simple approximation, the distributions look very similar to those presented in [19] that utilized an advanced Monte-Carlo code. The Monte-Carlo based distributions are wider for larger mean values of ν, when the contribution of secondary electrons become more important. For simple prediction of ionization distributions, e.g. for detector design purposes, the Poisson approximation can be valuable. For large values of d, especially when $d > D/2$, i.e. when the primary particle beam itself does not penetrate the sensitive volume, it is not so trivial to predict the distribution. For these large values of d, the $P_\nu(Q; d)$ values obviously drops dramatically and the detailed shape of the distribution at larger values of the impact parameter must be calculated by carefully simulating the tracks of the secondary electrons. Today, this is however a rather straight-forward procedure, see e.g. Ref [22].

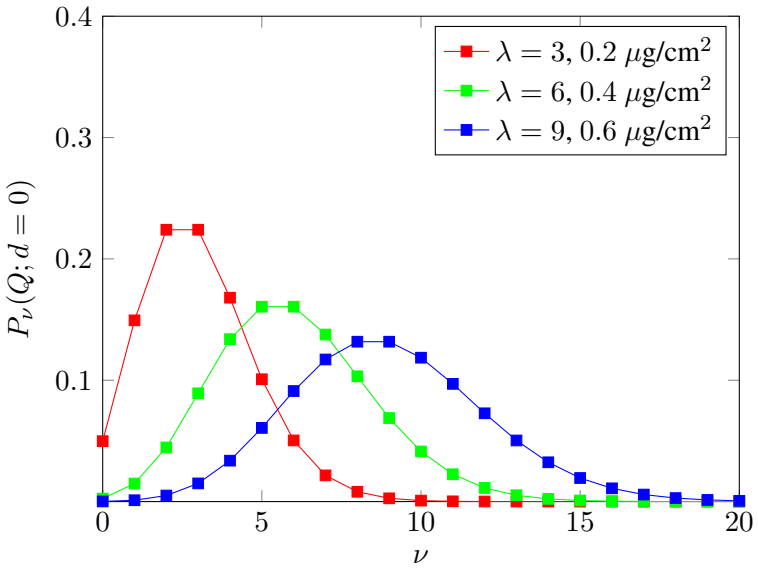

Figure 2.3: Probabilities, $P_\nu(Q)$, at $d = 0$, that exactly ν ions are detected, approximated by Poisson distributions. The parameter λ corresponds to the mean number of ionizations in the volume, and is roughly proportional to to the density of the cylindrical volume.

3 Detectors for micro- and nanodosimetry

A large spectrum of methods exists today for experimental micro- and nanodosimetry. One rational given to perform micro- and nanodosimetry measurements is to improve the ability to predict the biological effects (RBE) induced in living tissue by radiation of a various qualities. The microscopic quantities that e.g. focus on the spatial distribution of energy or ionization are considered to be superior in predicting effects in tissue compared to basic measurements of e.g. *absorbed dose*. In a recent review article [23], Palmans et al. argues that further improvements in measuring capabilities for both lineal energy distributions and ionization distributions is important for a better understanding of induced biological effects from various radiation qualities.

The *research* field of nano- and micro dosimetry is in itself important. Here, the main objective is to better understand the relationships between how radiation interacts with biological tissue on a microscopic level and biological effects over different time scales and to develop new ways of measuring and simulating interactions between radiation and matter at microscopic scales. Such understanding can, together with advances in technology, be used to construct new and improved micro- and nanodosimetry detector systems. On the modelling side, Monte Carlo-simulations have utilized the rapid development of modern computers and have been successful in investigating the relationship between ionization distributions and molecular-scale damage in biological tissue. Important advances in the experimental micro/nanodosimetry research have also been made in recent years, and some examples are given below.

At the same time measurements with micro- or nanodosimeters can be applied with different objectives. One group of application is monitoring detectors, to look at low-level doses to staff in e.g. aeroplanes or space-flight or in hospitals or nuclear power plans. Several medical applications exist, such as dose measurements in diagnostic treatments (e.g. PET, SPECT, CT) or monitoring and calibration of radiation therapy for different modes of therapy beams. The detector system must be chosen with care for each application, to account for the differences in e.g. dose rate, radiation quality, and radiation field geometry.

One of the long-term ambitions in experimental micro/nanodosimetry is to measure and map out the complete spatial track of ionization points in a (simulated) small volume. This is normally beyond reach for even state-of-the-art detectors today, but research projects using large prototype detectors in controlled radiation fields are already close to realizing track measurements with separated individual interaction points in simulated volumes at the nano-metre scale. Combining such track measurements with Monte-Carlo simulations could in the future enable models with a clear separation between the physics of the radiation interaction and the biological processes in living tissue, as discussed in Ref. [23]. While track measurements seems to be beyond reach for applied micro/nanodosimetry at the moment, it is important to keep track of this development, especially when considering practical detector development.

One objective for this prestudy is to make an overview of methods and detector tech-

niques used today in micro/nanodosimetry. In the following sections, after an overview of gas detectors and a brief discussion on semiconductor detectors, some focus is given to recent advances in the research of experimental nanodosimetry.

3.1 Gas detectors

In a typical gas detector, e.g. a proportional chamber of cylindrical geometry with a single central anode wire, and with a total voltage U between the wire and the detector walls, the electric field strength, E, varies as a function of the distance, r, from the anode wire as $E = U/r\,ln(b/a)$, where a is the anode wire radius and b is the inner radius of the detector. At a suitably low gas pressure this means that the charge multiplication in the gas takes place only in the high-field region where r is small, i.e. close to the anode. Only if this regional volume is small in comparison to the entire sensitive volume of the detector we can assume that the signal generated gives a good representation of the micro-dosimetric quantities such as lineal energy- or dose distribution. The need for such a multiplication region sets a limit on how low pressure (and therefore the simulated volume size) that can be achieved in the conventional single-event pulse-height technique. The need for charge multiplication is due to the fact that conventional TEPC:s using standard pulse-sensitive amplification are not sensitive to the exceedingly small charge pulses (down to a few individual electrons per event) that are to be collected at the anode when no multiplication takes place in the gas volume. No well-defined limit on the simulated size can be set here since it depends on the electrical and geometrical characteristics of the detector, and on the gas of choice, but there seems to be a consensus in that it is difficult to use gas multiplication in TEPC:s for microdosimetric measurements below a simulated size of 200 nm. Ref. [8] gives an approximate limit at a simulated size of 300 nm.

One important advantage of the variance(-covariance) method is that it does not suffer from the limitation discussed above. Providing a high-enough event rate, e.g. in a high radiation flux, no gas-multiplication is necessary. Using a gas detector with tissue-equivalent wall material operating at low gas pressures down to 15 Pa and detector sizes of a few cm:s, variance-covariance measurements have been performed with simulated sizes as low as 6 nm by Grindborg et al. in 1995 [24]. At this scale new limitations set in. One is the physical difficulty, as discussed above in section 2.4, related to the stochastic relationship between the number of ion-electron pairs and the deposited energy, i.e. the W-parameter, which becomes stochastic in nature at the nano scale. This problem is briefly discussed in the context of the variance technique in Ref. [24] and the authors refer to the calculation of Lappa and Bigildeev [25] as a possible way of handling this using correction factors that depend on the simulated object size. As discussed above, an alternative way to address the problem is to abandon quantities such as deposited energy and replace them by a formalism based on ionization distributions as discussed previously. Another difficulty is the level of electronic noise. This will not be discussed in any detail here, but will depend on several factors, such as the geometry of the gas counter, the anode geometry, the grounding, and the length and construction of the cable between the gas volume and the electrometer electronics. When considering a specific design in detector development, the expected noise generated should ideally be estimated beforehand.

3.1.1 Gas pressure and simulated size

The main idea behind using macroscopic gas detectors for dosimetric measurements on the micro- or nanometer scale, is the so-called *simulation principle*, the reasonable assumption that a low-density gas volume corresponds to a microscopic volume of tissue for biologically relevant observables, such as absorbed dose, lineal energy and ionization distributions.

We consider a high-energy particle with kinetic energy E penetrating a small spherical tissue volume with diameter d_t along the x-axis. The linear stopping power $|\frac{dE}{dx}|$ is denoted S. The mean energy loss of the particle in the tissue volume, ΔE_t, can then be written:

$$\Delta E_t = S d_t = \left(\frac{S}{\rho}\right)_t \rho_t d_t, \tag{3.1}$$

where $(S/\rho)_t$ is the (usually well-known) mass stopping power. The expression for ΔE_g, the mean energy loss in a spherical gas detector of macroscopic size is written in the corresponding way, replacing the t-for-tissue indices with g-for-gas. With the requirement for equal energy loss in the two volumes, i.e. $\Delta E_t = \Delta E_t$, we get:

$$\left(\frac{S}{\rho}\right)_g \rho_g d_g = \left(\frac{S}{\rho}\right)_t \rho_t d_t. \tag{3.2}$$

If we further assume that the atomic composition of the tissue volume and the detector gas are the same (i.e. when using a tissue-equivalent gas), and that the mass stopping powers are independent of density we see that the density ratio is equal to the inverse size ratio:

$$\frac{\rho_g}{\rho_t} = \frac{d_t}{d_g}. \tag{3.3}$$

For a certain detector size, d_g, we can now select a simulated tissue volume of our choice, d_t, by simply changing the gas pressure to correspond to ρ_g. The tissue density ρ_t is normally close to, and is sometimes put equal to, unit density: $\rho_t = 1\ \mathrm{g/cm^3}$.

It is worth noting that the macroscopic and microscopic volumes correspond to each other in some ways, but not in others. From above we know that the mean energy loss is the same for the two volumes. The volume ratio is $(d_g/d_t)^3$, but the mass ratio is $(d_g^3\rho_g)/(d_t^3\rho_t) = (d_g/d_t)^2$. Since the mean deposited energy is the same for the two volumes, this means that the ratio between absorbed dose from one single particle is $(d_t/d_g)^2$. On the other hand, since the ratio of the two cross section areas is $(d_g/d_t)^2$, the *dose rate* from particles in a homogeneous radiation field is the same for the detector as for the simulated volume. We see also that the area density (e.g. expressed in $\mathrm{g/cm^2}$) is the same for the two volumes.

To get some idea about the gas pressures relevant for this prestudy we can see what the typical gas pressures are for the simulated sizes of interest. Replacing tissue density with water density, considering a ionization chamber with diameter $d_g = 5\ \mathrm{cm}$, and aiming for a simulated volume of 1 μm, we get a gas density of $\rho_g = 1000\ [\mathrm{kg/m^3}] \cdot \frac{1\cdot 10^{-6}\ [\mathrm{m}]}{0.05\ [\mathrm{m}]} = 2.0 \cdot 10^{-2}\mathrm{kg/m^3}$. Using air as our gas (skipping the tissue-equivalent requirement for the moment) we have a density of $1.2\ \mathrm{kg/m^3}$ at 20 °C at the nominal atmospheric pressure of approximately $1\cdot 10^5$ Pa, and so the pressure in the gas detector should be $(2.0\cdot 10^{-2}/1.2)\cdot 1\cdot 10^5\ [\mathrm{Pa}] = 1.7\,\mathrm{kPa}$. If we are aiming for a simulated size at 10 nm instead, the gas density should be 100 times lower, i.e. 17 Pa. For gases that are not tissue-equivalent it is necessary to use scaling factors, and the above numbers will therefore change accordingly, although not dramatically.

3.1.2 Wall effects

Perhaps the biggest difficulty for variance-covariance measurements using standard tissue-equivalent ionization chambers at the nano scale are so-called *wall effects*. This term refers to signals generated due to events originating from scattering or reactions in the wall material of the detector volume. Ref. [8] discusses four types of wall effects: the *delta-ray effect*, the *re-entry effect*, the *V-effect*, and the *scattering effect*. The importance of each type of wall effect will depend strongly on the radiation quality. As an example the re-entry effect will be most important for electrons that might re-enter the gas cavity due to large-angle scattering in the wall material after the first interaction. The delta-ray effect corresponds to electrons being kicked out from the wall at the same time as the primary particle enters the gas volume. The V-effect refers to various nuclear interactions in the wall that could send two charged particles (rather than one) into the gas chamber at the same time. Ref. [8] notes that this effect could be important for neutrons above 10 MeV. It is likely that this could be an important effect for high-energy protons, of special interest in this report. The scattering effect is typically related to photons that interacts in the wall by Compton scattering or by scattering of neutrons.

All the above effects will give an overestimation of the average deposited energy, and in a variance-covariance measurement this would e.g. mean an overestimation of the $\bar{y}_D$ values. One type of low-energy delta-electrons is mentioned in Ref. [8] as a particularly limiting factor for variance-covariance measurements at low gas pressures. As the gas pressure is reduced towards simulation of nano-scale object sizes, the relative amount of low-energy electrons emitted from the walls increase. Electrons below around 30 eV are not able to ionize the gas to give false ionization events in the gas, but they will still contribute to the charge collected at the anode, giving an overestimation of the measured charge current.

In addition to the above effects related to interaction between radiation and the wall material we need to consider the effects of irradiation of all other parts of the detector system, such as the anode, the cables, and the connectors.

Some of the effects mentioned above is possible to correct for. A typical procedure in a variance-covariance measurement at low gas-pressure is to collect data also at full evacuation of the gas in the detector, i.e. at almost complete vacuum. The standard way of deducing the dose mean lineal energy would then be using the following expression, see e.g. Ref. [24]:

$$\bar{y}_D = \frac{((V_m/Q_m^2 - C_r)Q_m^2 - V_b)W/e}{(Q_m - Q_b)\bar{l}}k, \tag{3.4}$$

where V_m is the measured charge variance and Q_m is the measured mean charge and V_b and Q_b are the corresponding measured quantities at zero gas pressure. We have also the relative covariance, C_r, a constant conversion factor, k, and the parameter W, discussed elsewhere in this report. As pointed out in Ref. [24], the resulting statistical uncertainty of $\bar{y}_D$, using this background correction procedure, is typically dominated by the uncertainty in the measured variance. For smaller simulated object sizes the increasing uncertainty of V_b and C_r of equation 3.4 will generate larger errors. A large number of integrations (i.e. a longer measuring time) in the measurement reduces the relative uncertainty of the relevant quantities. For cases where the fluctuating background signal is considerably more intense than the signal of interest the method will fail to give a meaningful value for $\bar{y}_D$.

Simplifying the above expression by assuming a constant radiation field (so that the covariance part becomes unnecessary), and assuming a constant W, we can write:

$$\bar{y}_D = \frac{V_m - V_b}{d(Q_m - Q_b)}c, \tag{3.5}$$

where d is the simulated size and c is a constant. Using the method above to correct for the background (the behaviour of the detector system at zero gas pressure) *some* of the mentioned effects could be corrected for, such as the low-energy electrons entering the gas volume and, to some extent, the irradiation of the anode, cables or connectors. Other effects will not disappear, such as high-energy delta-ray electrons giving unwanted additional ionization at nano/micro-scale gas pressures, but not at total vacuum. Another remaining problem would be the V-effect, in particular for high energy protons, neutrons, and heavy ions. It is clear that a good understanding of wall effects are necessary to avoid mistakes in measuring with walled gas detectors at the nano scale. The wall effects typically give (often unknown) systematic error, rather than statistical fluctuations and will therefore affect variance-covariance measurements in a problematic way. Detailed Monte-Carlo simulations of the particle interactions in the detector walls is an attractive way of addressing this and a lot of work has been done in this field, but will not be discussed here.

The two most common geometries used for the sensitive volume of micro-dosimetric gas-filled detectors (typically TEPC:s or mini-TEPC:s) are the *sphere* and the *cylinder* [8]. While the spherical detectors have an appealing symmetry for the sensitive volume itself, the anode collecting the charge pulse is typically a straight wire, stretched over the diameter of the sphere so that the electric field near the anode has a cylindrical symmetry. Often additional electrodes (e.g. helix wires) are added to shape the electric field inside the spherical volume. In a cylindrical detector the anode wire is normally situated at the symmetry axis of the cylinder and additional field shaping is not needed as the gas volume and the electric field share the same symmetry. As noted by e.g. Kellerer (Ref. [8], p. 80), for isotropic radiation, a cylinder with its diameter and height equal has the same mean chord length as a sphere with the same diameter. This particular cylindrical shape is therefore commonly used both in detector design and in simulations.

3.1.3 Wall-less detectors

A detailed review of the various designs of wall-less detectors for microdosimetry was written by Glass and Gross in 1972 [26]. The wall-less gas detectors designed for micro- and nanodosimetry can be categorized in two types. One approach is to shape an electric field in such a way so that the field lines define the volume. A few examples are discussed in Ref. [26]. Modern example of this approach used for nanodosimetry are discussed in sections 3.3.1 and 3.3.3 below. General disadvantages of this approach is that the sensitive volume in the electric field is often difficult to define well and that the shape and size of the volume and its boundary are very sensitive to small fluctuations in the electrical environment [8].

A second approach to make a wall-less gas detector is to build a wall from a sparse grid made of thin wires of metal or other materials, such as conductive tissue-equivalent plastics. If the wires are thin and the grid is sparse, only a small fraction of the shaped area is occupied by material. A spherical gas detector of this type was used, and is

briefly described, in Ref. [27]. It uses a wire grid made of tissue-equivalent A150 plastic. This detector currently resides at SSM in Stockholm and will be part of future planned test experiments, see section 4.1.3. In general, the wire-type wall-less detectors have the advantage of having a well-defined sensitive volume, and they can be made quite robust. A disadvantage is that they are not truly wall-less, since a small amount of material is still present at the boundary of the sensitive gas volume.

An important advantage of wall-less gas detectors, as compared to standard ionization chambers, is that the influence of some of the wall effects can be removed or reduced. As discussed above, in particular the influence of low-energy secondary electrons can be a limiting factor in measurements using the variance method at the 10 nm scale, since the uncertainty of the variance in the background measurement becomes too large. Such influence can be dramatically reduced using a wall-less detector, for example of the type presented in Ref. [27], where the electric field can be arranged so that the low-energy secondary electrons do not enter the sensitive volume.

3.1.4 Parallel-plate detectors

Not much is found in the literature about micro-dosimetric gas detectors with a parallel plate geometry. The reason for this is most likely the dominance of the single-event (pulse-height) measurement technique with the need for a high electric field strength near the anode. It is e.g. telling that parallel-plate designs are not mentioned at all in the detector design reviews in Refs. [8] and [26]. For measurements approaching the nanometer range using the variance method a common procedure has so far been to use a (spherical or cylindrical) detector designed as a proportional chamber (using the pulse-height technique) for variance measurements without gas multiplication at very low pressures. Apart from the aspect of flexibility in application, this has had the advantage that the results of the two methods could be compared to each other at simulated sizes above around 0.3 μm where not only the pulse-height technique, but also the variance method could utilize gas multiplication.

With a parallel plate design the sensitive volume boundaries are defined by the shape of the two electrodes. We can for example get a rather well-defined cylindrical shape of the sensitive volume by mounting two electrodes of circular shape parallel to each other. While not suited for the single-event method, parallel plate ionization chambers should work well for variance-covariance measurements. For some applications, e.g. in a therapy accelerator beam geometry, there are additional advantages to such a parallel geometry.

In Ref. [28], Forsberg and Lindborg successfully measured $\bar{y}_d$-values in a field of ^{60}Co γ-rays using a parallel-plate ionization chamber with the variance technique down to simulated sizes of around 20 nm. The detector geometry was however intentionally not optimized to achieve a good result for $\bar{y}_d$. Instead the geometry allowed the γ rays to enter the device mainly through one of the two plates. The objective was to investigate how the relative contribution of secondary electrons emitted from the electrode affected the measurement. Around 20 nm, the current from secondary electrons was found to be comparable in amplitude to the ionization current, making the $\bar{y}_d$-values unreliable. This is a valuable result, since it allows us to estimate the influence of the wall effect from secondary electrons for various geometries.

Possible designs for parallel-plate detectors suitable for the variance technique in nanodosimetry are discussed in section 4.2

3.1.5 Approaching the limits at the nano scale

Some effort was made during this prestudy to find out what the main limiting factors are for reaching small (nanometer scale) simulated volumes with a tissue-equivalent gas-filled detector. While no definite/simple answer can be given, a few hints can be found from earlier published studies. Two relevant articles are presented below.

In 1989, Lindborg et al. investigated systematic and statistical uncertainties in measurements using the variance-covariance technique [27]. They measured $\bar{y}_D$ in a neutron beam at 5.7 MeV down to a simulated object size of 20 nm. The results and discussion give some hints on how to reach even smaller object sizes. First, the results achieved using the variance technique are in agreement with results from the pulse height method in the range 300 nm to 3 μm. At lower gas pressures, where only the variance method could be used, values for $\bar{y}_D$ with statistical errors below 8% were measured at 100 nm, 30 nm, and 20 nm. At 10 nm the results were considered unreliable due to a large variation between runs. The authors refer to an earlier experiment where they reach the limit at 50 nm. Several improvements were made to the detector setup between the two experiments, reducing noise sources of different origin, in order to reach the 20 nm limit. The authors note that the limiting factor in the presented experimental setup was the insufficient shielding of the preamplifiers. But they also point out that the by far most important improvement was the larger detector *sensitivity* in the newer measurement. The meaning is that the electric current originating from micro-dosimetric ionization in the gas was increased in comparison to the summed contributions of (noise) current, including electronic noise. The ionization current from a spherical detector of macroscopic radius r, for a simulated diameter d, and for a dose rate D is:

$$Q/t = kdr^2D, \tag{3.6}$$

where k is a constant and Q is the electric charge measured over an integration time, t. We note that the current increased quadratically with the detector radius, r. If, as in the study in Ref. [27], the limiting factor is noise contributions from a preamplifier, one could improve the measurement simply by increasing the detector size. With this argument the authors claim that a simulated size of 2 nm could be reached if the detector radius was increased from 2.5 cm to 8 cm. One should however be aware that (depending on the detector design) some noise contributions also could increase quadratically as a function of the radius. One would for example expect secondary electrons emitted from the walls in a walled spherical detector to increase approximately with r^2.

In 1995, Grindborg et al. used the variance-covariance technique to measure the dose mean lineal energy, $\bar{y}_D$, for simulated diameters down to 6 nm [24] using both 1173 keV and 1332 keV γ-photons from a ^{60}Co source and from an X-ray beam (voltage 100 kV). Low-noise electrometer electronics were used. At the smallest simulated sizes the relative error of $\bar{y}_D$ was around 25% in the gamma measurement and considerably larger for the X-rays. The authors conclude that the lower limit for simulated object size with the presented experimental setup is around 9 nm. A discussion about uncertainties and their origin is made in the article. For the X-ray measurement a large covariance term was a serious problem at the smallest object sizes, perhaps related to fluctuations in the X-ray source. For the γ-rays the covariance was less of a problem, but still quite noticeable at around 10-30%. One parameter contributing to the covariance is fluctuations in gas pressure. The most serious limitation for both radiation modes was however the background variance, V_b. This (approximately constant) value became larger than the

micro-dosimetric variance, V_m for simulated object sizes below 10-15 nm. This, in combination with the uncertainty of both V_m and V_b sets the limit of measuring $\bar{y}_D$, as seen in equation 3.4. The authors also note that the X-ray measurement was limited by electronic noise, but that the ^{60}Co γ ray measurement was limited by secondary electron emission.

3.2 Semiconductor detectors

Since the 1970s, there has been an interest for using semiconductor devices as detectors in microdosimetry. Typically a pn-junction diode of some kind has been used. As an example, lineal energy distributions for fast neutrons and gamma radiation was first measured using a silicon photo-diode by Orlic et al in 1989 [29]. Early applications of semiconductor devices include microdosimetry in proton therapy at simulated sizes around 10 μm [30]. The interest for solid state devices used in microdosimetry has risen rapidly in the last two decades. This has coincided with new and cost effective methods of manufacturing solid state components, driven by the computer- and information technology industries.

There are several advantages of using silicon based microdosimeters compared to conventional gas detectors such as TEPC:s or ionization chambers. The solid-state devices themselves are very small and light. Several dosimeters are easily put on the same chip for increased efficiency. At the same time this enables position resolution in the micrometer scale for e.g. beam diagnostics. Silicon-based microdosimeters could also be combined with other sensors or other solid-state hardware on the same chip. the power consumption is low, and no high voltage or controlled gas pressures are needed, making the detectors quite flexible in use and able to withstand rough environments. The devices could potentially be manufactured at low cost in high numbers. It is likely that Si-based microdosimeters will start to replace TEPC in a number of applications in the not-so-distant future, especially in high-LET fields such as in radiotherapy or aerospace applications.

A popular detector type is the silicon-on-insulator (SOI) device. The SOI designs has the advantage that charge collection is blocked from underneath the active Si device due to the insulator substrate. This makes the sensitive volume well defined. In the review in Ref. [31], five generations of silicon based microdosimeters are described. The focus is on SOI but also microdosimeters based on miniature $\Delta E - E$ telescopes are presented. The $\Delta E - E$ method is a long-standing standard technique in experimental nuclear- and particle physics that enables the discrimination between different charged particles, e.g. protons and α-particles, in a mixed radiation field. When several micro-scale Si-telescopes are mounted on a chip it is possible to combine the particle discrimination with a multi-array micro-dosimetric measurement.

While not discussed in the review of Ref. [31], the above mentioned silicon dosimeters has a few drawbacks and challenges. One difficulty is to find relevant corrections for tissue inequivalence of silicon. Another is the (at present) limited ability to measure low-LET radiation. Today, the lower LET limit for the best SOI:s is 0.6 keV/μm [31]. This makes measurements of lineal energy distributions in gamma- and electron fields difficult. Yet another drawback is the relatively large simulated size. Silicon devices simulate sizes in the same order-of-magnitude as the real size of the sensitive silicon volume. While this is an attractive feature in itself it does limit the range of the simulated size considerably. For all devices discussed in the overview of Ref. [31] the sizes

of the active individual silicon volumes are around 1 micrometer or larger. Therefore these modern standard silicon-based microdosimeters are of limited interest for this particular prestudy, since we are focusing on the nanometer scale.

However, a few attempts to explore dosimetry in solid-state-based devices at the nanometer scale using the variance technique has in fact been made [32, 33, 34].
Burlin [33] suggested that secondary electron emission from a thin surface layer into a gas volume could be a way to extract relevant dosimetric data on the nanometer scale. The idea is based on the fact that the low-energy secondary electrons have a range in typical wall material in the order of 10 nm. Collecting the charge of these secondary electrons (from transmission or reflection) in the gas detector would then give information on nano-scale interactions in the wall material. This was explored in some detail in an article by Forsberg and Burlin in 1980 [34] where experimental data and model simulations are compared. The results include e.g. $\bar{y}_D$ values for object sizes of 10 nm and some aspects related to biological effects are discussed. The method obviously lacks the flexibility of selecting the simulated size by adjusting the gas pressure. Instead, different materials (or, possibly, different microscopic structures of the surface) would correspond to different object sizes.

3.3 Recent advances in experimental nanodosimetry

Interesting development in the field of experimental nanodosimetry has been seen in the last two decades. This has partly been triggered by the advances in Monte Carlo simulations of particle tracks in the vicinity (measured in nanometers) of biological structures sensitive to radiation, such as DNA-molecules. By comparing such simulations with measurements in simulated volumes of sizes of the same order of magnitude, new relevant ways of relating radiation quality to biological effects are appearing. A common formalism today when comparing experiments and simulation and when discussing their biological relevance is based on ionization clusters, as described above in section 2.5.

Three projects stand out as examples of modern experimental setups in experimental nanodosimetry: The *Ion Counter* setup at the National Metrology Institute (PTB) in Germany, the *Jet Counter* project at the National Centre for Nuclear Research in Poland, and finally the *STARTRACK* apparatus for track-nanodosimetry designed at Legnaro National Laboratories in Italy. The STARTRACK setup is here described in a little more detail than the other two, as an illustrative example of modern nanodosimetry research.

3.3.1 The PTB Ion Counter

The Ion counter at PTB, Germany was originally designed at the Weizmann institute of Science in Israel [35]. In this device, charged particles (typically protons, α particles or heavier ions such as $^{12}\mathrm{C}$), traverses a low pressure gas volume, ionizing the gas. The walled gas volume measures about 26 cm across, but a smaller wall-less volume is defined by an electric field that is able to extract the ions from the gas, through a small aperture into a detection volume at lower pressure, where an ion counter is registering individual ions and record their time of impact. The primary beam particles hit a trigger detector after leaving the gas volume so that the detected ions can be correlated with an individual primary particle. In this way the ionization cluster size distributions can

be acquired over time. The wall-less volume defined by the shape of the extraction field correspond to the simulated size of interest. With propane gas at a pressure of $1.2 \cdot 10^{-3}$ bar, the diameter of this volume correspond to a distance in liquid water of approximately 3-4 nm, while its height is around 90 nm [19].

High-quality simulations of the ion extraction efficiency as a function of position in the electric field are crucial to define the sensitive volume with high precision. Several technical challenges exists and the count rate is quite limited. Nevertheless, ionization cluster distributions agree well with Monte Carlo simulations for cluster sizes from 1 up to around 20. The results are quite sensitive to parameters in the electric fields, even in the field in the detection volume after the extraction [35].

3.3.2 The Jet Counter project, Poland

The Jet Counter project in Poland [36] uses pulse expansion of a gas, generating a nitrogen gas jet of very low density in a cylindrical interaction cavity with diameter and height both equal to 10 mm. A fast piezoelectric valve is used to perform the pulse expansion. The cavity has 1 mg/cm^2 Mylar walls. The primary particle penetrates the cavity and is detected on the other side by a trigger device, a Channeltron B419 BL. An open bottom in the interaction cavity and grid potentials generating an electric field enables extractions of individual ions accelerated towards a AF180H ion detector. Each incoming primary particle can then, similarly as for the PTB Ion Counter, be correlated with an ionization cluster size. Potential wall-effects from the Mylar walls of the interaction cavity and a low counting rate are some of the challenges for this device.

Unlike the two other nanodosimetry experiments discussed here, the Jet Counter is designed to be able to measure low energy electrons, even in the range below 3 keV where applications in Auger electron radiation therapy exist. Results for ion cluster distributions from 100 eV to 2 keV have been presented [37].

3.3.3 The STARTRACK experiment at LLNL, Italy

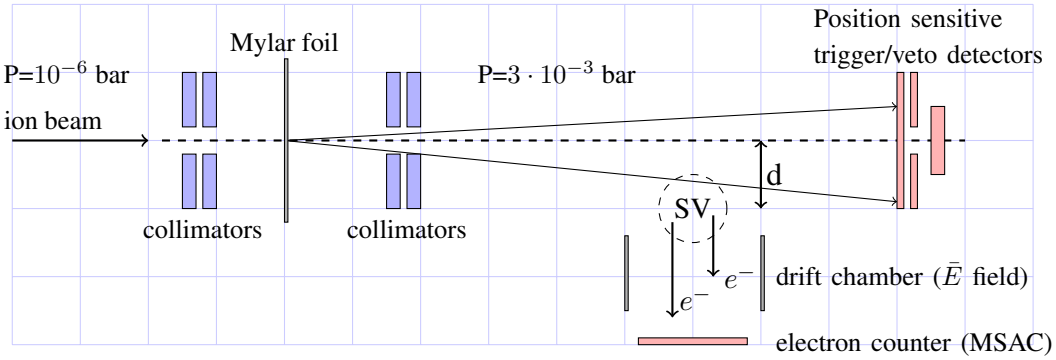

Figure 3.1: A schematic illustration of the STARTRACK detector setup. Individual particles of the ion beam is collected by trigger- and veto detectors to monitor the path of the primary particle. The wall-less sensitive volume (SV) is defined by the electric field collecting electrons through the drift chamber. The parameter d can be controlled by adjusting the field geometry.

The STARTRACK apparatus [38] at Legnaro National Lab in Italy is designed to measure ion cluster-size distributions at the nanometer scale by detection of individual electrons from ionization events in a low-pressure gas volume. The device is at present the only one of its kind in operation. A schematic picture for illustrating the detector principle i given in Fig. 3.1. Several details have been left out, such as the complexity of the veto- and trigger system. The operational principle is briefly explained here. The collimated ion beam (typically protons or heavy ions) approaches the device from a low pressure region (10^{-6} mbar) and enters the gas-filled region (propane gas at 3 mbar) through a Mylar window of $1.5\ \mu\mathrm{m}$ thickness. The primary particle then passes (through or nearby) the wall-less sensitive volume (SV) and is then detected downstream in the trigger/veto detector array. By the position-sensitivity of the trigger/veto system, the impact parameter, d, i.e. the distance, from the symmetry axis, at which the particle passes the centre of the SV, can be controlled and unwanted scattered events can in addition be removed from the acquired data stream. The SV is defined by the shape of the electric field that transports (in a direction perpendicular to the beam axis) the free low-energy electrons liberated at the ionization sites of the gas. A long (20 cm) drift chamber is used to slowly separate the *individual* electrons in space and time-of-impact in the multi-step avalanche chamber (MCAP) electron counter. In this way, the exact number of created ion-e^- pairs, correlated to each primary particle can be counted. After several such collected events, a $P\nu(Q,d)$ distribution is acquired. The impact parameter, d, can be changed by controlling the electrical field defining the sensitive volume, SV.

The average efficiency for the extraction of electrons from the SV is about 25%, but this number depends on the exact position in the gas volume, and in this sense the boundaries of the SV are not well defined. A number of experiments with simulated object sizes in the nanometer range has been performed, with different primary (charged) particle beams and with several different impact parameters [18]. One example is the experiment presented in Ref. [21] where a gas pressure corresponding to a SV of 20 nm was used and where the primary particle beam consisted of 20 MeV protons and the experimental impact parameter was fixed at 0.5 mm corresponding to a simulated impact parameter of $d = 2.7$ nm. The resulting P_ν distribution is presented and compared with a Monte Carlo simulation, giving excellent agreement in a wide range between $P_0 \approx 0.8$ and $P_{12} \approx 10^{-5}$. For cluster sizes above $\nu = 12$ the low counting rates gives large statistical fluctuations. One problem encountered is low-energy (delta) electrons that spontaneously enter the drift chamber and give an unwanted background since these electrons, uncorrelated to the ionization in the SV, are also detected by the MCAP. This effect is seen for $\nu > 6$ and is handled by measuring with the beam on but with the field forming the SV turned off. The unwanted contribution can then, by a simple procedure [21], be subtracted.

This result, and others using the same equipment, shows clearly that individual ion-e^- events can be counted in a wide P_v distribution range at the nanometer scale, down to individual ionization events ($\nu = 1$). Developments of the presented techniques will involve a more advanced extraction of electrons from the sensitive volume with the potential to give more detailed spatial information from the ionization tracks.

4 Nanodosimetry at SSM

4.1 Existing infrastructure and detectors at SSM

4.1.1 Sources

The Swedish secondary dosimetry laboratory (SSDL) at SSM [39] use a number of radiation sources, mainly for reference/calibration purposes. Of particular interest for the present work is a ^{60}Co gamma source (activity 440 TBq in Dec. 2012) used for calibration of radiation therapy instruments. It can produce a field with a Kerma rate in air of about 16 mGy/s. A number of intense X-ray fields (60-3100 μGy/s) for similar purposes are also available at SSDL. In particular the gamma field (more stable than the X-ray fields) would be a good place to start for performing new variance measurements at the nano scale, testing different detector designs.

4.1.2 Electronics

Several generations of electrometer electronics for dosimetry exist at SSM. Much of this electronics has been designed and built at SSI/SSM, by G. Samuelsson and others. The devices *Apparat 1*, *Apparat 2*, and *Elektrometer 3* have all been used in reference/calibration measurements at SSDL/SSM (formely SSI). The implementation of an updated version called *Elektrometer 4* has recently been discussed. A pair of electrometers called *Elektrometer A&B* was developed at SSM providing low-noise electronics for measurements down to the nanometer range. These electrometers and their readout electronics still exists at SSDL/SSM and are described in some detail in Ref. [24]. More recently, modern commercial electrometers are also used at SSDL/SSM. In addition, the so-called *Sievert instrument*, described in detail in Ref. [6], is used for various field measurements by the SSM staff. It includes both detector- and electronics hardware. The instrument consists of two separate detectors cavities, enabling the use of the variance-covariance technique in non-constant radiation fields. Independent of this prestudy there are some plans at SSM to upgrade or replace parts of the Sievert instrument (e.g. high voltage, electronics, ACQ-readout).

4.1.3 Detectors

A number of detectors that are relevant for future measurements with the variance technique already exist at SSM. Some of these are designed as proportional chambers, although they can also operate without gas-multiplication at low pressure. The two most common wall materials for these detectors are the tissue-equivalent A-150 plastic, and the air-equivalent C-522. The Sievert instrument, see above, includes two gas detectors with 5 mm thick A-150 wall material and a 2 mm thick aluminium casing. A number of older gas detectors are also available, such as the Extradin models A6 and A3, the latter of which was used in the experiment in Ref. [24], both with C-552 plastic wall material. A number of smaller/miniature ionization chambers of different sizes also

exist. Of particular interest for the present work is a wall-less detector borrowed from Columbia University. It is described in Ref. [27]. The wall-less volume is defined by a spherical grid of A-150 material with a diameter of 51 mm and a transparency of 85-90%. The central anode is surrounded by a helix-shaped wire with a helix diameter of 6.4 mm. The above is only a selection of interest for this study. Several additional older ionization chambers, some designed at SSI/SSM, are also available.

4.2 Ideas for detector development and tests at SSM in the near future

In the following subsections follows some ideas of possible measurements and detector development at SSM to reach further in establishing the variance method at simulated volumes of 10 nm or below. Since the infrastructure to perform measurements in intense low-LET photon fields already exists at SSM, it would be natural to start with such measurements and with the experience gained from that perform measurements in e.g. proton beams as a second step.

4.2.1 Gas detectors for variance measurements

4.2.1.1 Measurements with existing gas detectors

Three types of existing detectors are of interest here.

- First, the Extradin detectors with air-equivalent walls can be used to repeat the measurements performed by Grindborg et al. in 1995 [24]. Here, the same electrometers (*Electrometers A&B*) used in the original experiment can be used, but should also be compared to modern commercial electrometers. Especially the noise level and contribution to the background variance signal in low-current measurements is of interest. Both the ^{60}Co source and one of the X-ray sources could be used in such measurements. For measurements in the ^{60}Co gamma field, there should be no need for a covariance measurement, so only a single detector is needed. This is under the requirement that the gas pressure fluctuations are small and measured/recorded continuously.

- Second, the wall-less detector from Columbia University [27] should be tested in the photon fields at SSM. One would expect to see a reduction in the influence of secondary electrons compared to the Extradin detectors, due to the different design. This and the above detectors have similar dimensions, so in both cases a pressure around 15 Pa corresponds to a simulated size of 10 nm. The detector consists of a solid outer enclosure/wall, a sparse wire grid of spherical geometry, a helix wire enclosing a central cylindrical volume, and a thin central anode wire. Ref. [27] gives some detailed information on how the relative electrical potential of the helix wire compared to the grid potential influences the electrometer current. By adjusting these potentials, one has the option of using the inner cylindrical volume, enclosed by the helix wire, as the sensitive volume for the measurement [40].

- Third, the miniature ionization chambers at SSM should be tested in the low-LET field of the ^{60}Co source. There are already some plans to use these detectors for

variance measurements in a proton field, and the gamma field measurement is a good preparation for this. The influence of the small volume and relatively thick walls compared to the larger detectors is of high interest here. The gas pressure for these small detectors should be higher. As an example, the Wellhöfer ionization chamber, model F23-C with air-equivalent thimble, has a sensitive volume of 0.23 cm^3, and to simulate a 10 nm object would require a gas pressure at around 100 Pa.

4.2.1.2 Larger spherical tissue-equivalent and wall-less gas detectors

As discussed in section 3.1.5, a way to reach smaller simulated volumes in the nanometer range with the variance method is to increase the diameter of the detectors. As an example, compared to the Extradin and Colombia detectors above with an approximate diameter of 5 cm, a detector of 25 cm diameter at the much lower air pressure of around 3.3 Pa would simulate a water volume of 10 nm size. Such a detector could be designed based on the design of the above-mentioned wall-less Colombia detector, to investigate the effect on the ionization current compared to noise contributions of different origin, including the electrometer electronics and secondary electrons.

4.2.1.3 Large parallel-plate gas detector

As discussed in section 3.1.4, it seems that parallel detectors are under-exploited in variance measurements at the nanometer scale. Perhaps the highest potential for this approach lies in proton beam applications, but some investigations could be done in a high-energy photon beam as well.

A large parallel plate detector designed for measurements in the intense $^{60}\mathrm{Co}$ field at SSDL/SSM could be used to test the potential advantages of the parallel-geometry design. The detector could e.g. have a cylindrical geometry with two circular parallel plates, e.g. with radius 10 cm and inter-plate distance 10 cm, possibly with a variable plate-to-plate distance. The exact design of the cathode/anodes needs extra care to avoid generation of electronic noise. The detector walls should be made of standard tissue-equivalent plastic surrounding the low-pressure volume. A constant electric field is generated by a high voltage between the plates. This simple device could then be situated in the photon field in two different ways, illustrated in Fig. 4.1. In the first case, (a), the photon field encloses the whole detector, while in the second case, (b), only part of the inter-plate volume is irradiated by the primary photon field. In both cases, a large fraction of the ionization of the gas will be due to high-energy secondary electrons produced by both Compton scattering and photo effect interactions in the tissue-equivalent wall material. Especially due to the large-angle Compton scattering events, the geometry in (b) does not correspond to a detector operating wall-less mode. However, the total effect of the direct and indirect irradiation of the anode and cathode plates will be smaller for case (b), and therefore the comparison can be used to study the influence (e.g. secondary electron emission and electric noise contribution) from the anode/cathode irradiation at low gas pressures. This would enable us to investigate the influence on Compton scattering and secondary electron emission from the anode/cathode plates.

Moreover, due to the field-detector geometry, and since a narrow field cone could be moved away from the symmetry line in a controlled manner, one could attempt to measure impact-parameter-dependent currents using the variance method. This should

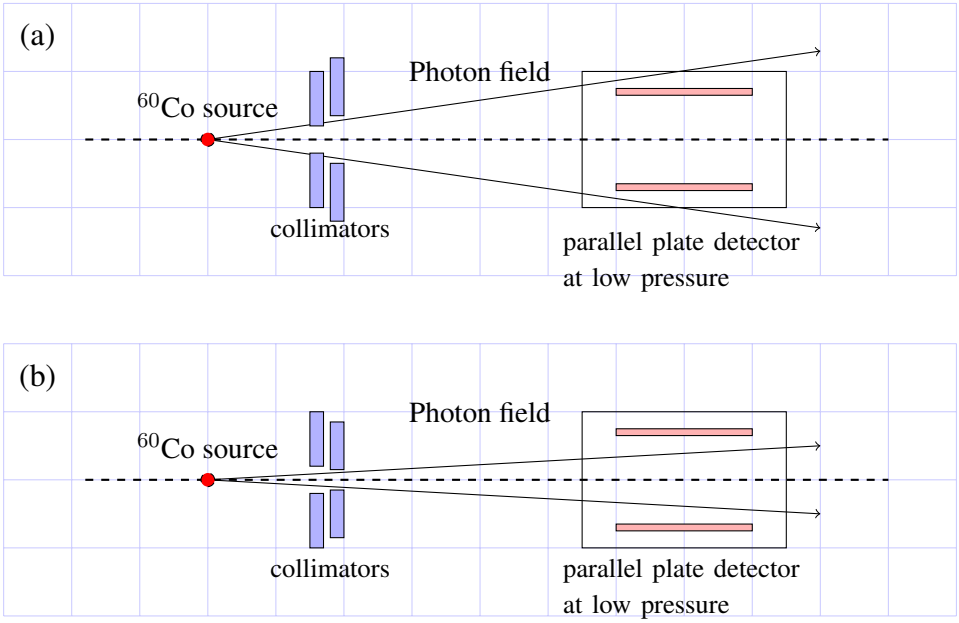

Figure 4.1: A schematic illustration of a parallel-plate detector in a high-energy photon field. The field geometries in (a) and (b) are both of interest.

in principle be possible since the energy-dependent Compton angular distribution (for the scattered electron) after interaction, although not narrow, is forward-focused and easily predictable by Monte Carlo-simulations. If meaningful results would come from such a measurement it could potentially allow for testing the simulations and single-event measurement of ionization distributions in the $P_\nu(d)$-formalism, see section 2.5, using the variance method for the first time. Measurements with a large parallel-plate ionization chamber could in this way complement and extend the above-mentioned measurements with existing detectors. By the results, and by comparing with simulations, a better understanding would be gained on the limitations of the variance method using gas detectors for simulating objects around the 10 nm scale.

The parallel-plate detector geometry discussed above could also be combined with a sparse grid of metal or tissue-equivalent plastic placed inside the walls of the low-pressure region, forming a wall-less design, thereby limiting the influence of low-energy secondary electrons.

4.2.1.4 Parallel plate detector in accelerator beam geometries

For applications with a beam-type geometry, i.e. in accelerator based proton therapy, a parallel-plate detector geometry give the potential of a (effectively) wall-less detector with charge collection on one of the plates. Unlike the gamma photon case, one would expect a considerable fraction of the current to originate from direct interaction/ionization between the beam and the gas atoms. Due to the constant electric field in this geometry, no gas multiplication is possible, but also not needed when using the variance method. To complement the planned measurements with a miniature ionization chamber in a proton field, a small parallel detector (e.g. a cylinder geometry with 2 cm plate gap) could be used, for which the primary proton beam passes through the

wall-less symmetry axis. It should be vital that the plate-gap is large enough to avoid beam halo or a large fraction of scattered beam to directly hit the anode/cathode plates. For such applications it is likely that scattered beam will be of high influence, and Monte Carlo simulations of the experimental setup could be very useful.

4.2.2 Alternative detector designs

4.2.2.1 MCP-based gas detectors

In early discussions in the present work a suggestion was made by C. Iacobaeus at SSM to use multi-channel plates in a parallel geometry with a low-pressure gas as a detector at the nanometer scale. This idea is briefly discussed here.

The gas cavity of the detector would here correspond to the parallel geometries discussed above. Gas multiplication in the sensitive gas volume should not be used, and would not be an issue at the low pressures relevant for the nanometer scale measurements. The difference to the above parallel-plate detector design is that the anode plate is replaced by a multi-channel plate (MCP), see Fig. 4.2 This device is sensitive to incoming electrons and by electron-multiplication in microscopic channels the charge-signal is directly amplified in the MCP by many orders of magnitude (a typical amplification factor would be 10^4). It is common in modern commercial MCP detectors to combine two MCPs in series, in a so-called *Chevron* design, where the angled channels of the first MCP is rotated 180° compared to the second MCP. This reduces ion feedback and allows for an even larger amplification.

In principle such an MCP setup could be used both with the single-event/pulse-height method, and with the variance method. For the variance method, a big advantage is that the charge signal is amplified far above any noise level that could be a problem for a traditional anode-based setup. Another advantage is that the MCP is position-sensitive (with inter-channel distances in the order of 10 μm. This could e.g. be used to divide the readout in two separate parts for variance-covariance measurements, effectively using one single detector as two. In single-event mode, the position resolution has the interesting potential to get more detailed spatial information from the ionization tracks in the gas volume. An optional trigger detector downstream from the gas cavity could reduce noise significantly in a beam geometry. Such setup is similar to e.g. the STARTRACK experimental setup presented in section 3.3.3. A drawback with a triggered detector is that it would add to the detector size and limit the count rate considerably. Modern chips that enable fast readout from pixelized detectors exist today and could possibly be combined with a MCP detector of the above type. One example is the *Medipix* CMOS chip [41] developed at CERN.

The MCPs are designed to be used in vacuum. A serious challenge to be addressed for the present application is the maximum pressure limit at which the device can operate reliably. Typical quoted maximum pressures for MCPs are 10^{-5} to 10^{-4} [Torr] [42], i.e. 1.3 [mPa] to 13 [mPa]. At higher pressure the noise level will increase and there is a danger of damaging electron feedback or electrical breakdown [42]. The above pressures should be compared with typical gas pressures in the order of 10 Pa for a detector of diameter 10 cm simulating an object of 10 nm. There could be ways to address this, including using differential pumping to create a pressure grading between the sensitive volume and the MCP, or experimenting with the electric field gradient above the MCP, but such methods involve a number of difficulties in design and method. There is also a risk that the detector would be large and perhaps complicated to use. Nevertheless,

while several technical challenges remain, an MCP-based detector has the long-term potential of nanodosimetry measurements based on ionization track analysis. A device similar to MCPs is the gas electron multiplier (GEM). It could also have potential use in track-dosimetry in the future.

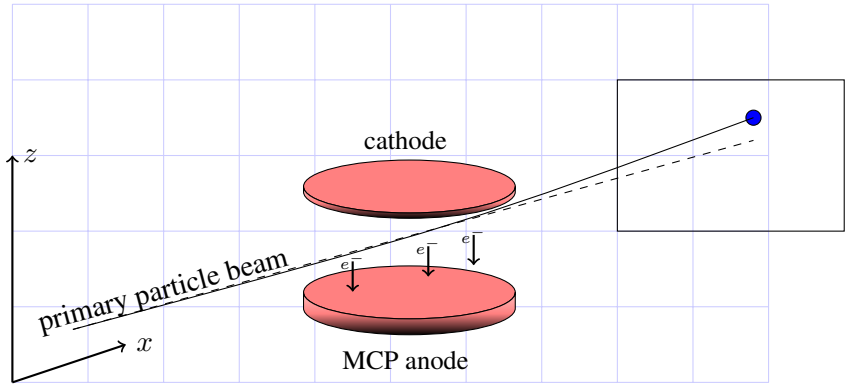

Figure 4.2: A parallel gas detector with an MCP anode. The primary beam could optionally be collected at a trigger detector.

4.2.2.2 Detectors measuring secondary electron emission

The potential to use secondary electron emission from the inner walls of an evacuated gas-detector as a means to study the ionization probabilities and energy deposits in various wall materials was briefly discussed in section 3.2, see also Ref. [34]. While such measurements have the potential to approach the 10 nm-range of simulated volumes, the detector principle has several limitations. As an example, the simulated size cannot be chosen by simply changing a gas pressure, but instead statically depends on the material of choice. Another difficulty is that the simulated volume in a measurement using this method is not well defined, since the individual electrons entering the inner detector volume have started from different depths in the wall. This problem, while non-trivial, could in principle be handled, e.g by using an *effective* simulated volume deduced from careful Monte Carlo simulations. Since secondary electron emission is of interest for a better understanding of background noise and limiting factors in future measurements with gas detectors, it might be a good idea when studying these noise signals to investigate the potential of this particular detector principle at the same time. This could be done with both Monte Carlo simulations and measurements.

4.3 Formalism and Simulations

4.3.1 Impact-dependent formalism for variance measurements

As discussed in section 2.5, the results from measurements of ionization distributions at the nanometer scale requires an alternative formalism if the geometric relationship between the incoming particle and the detector is to be taken into account, and if the ionization distribution is the observable in focus, rather than deposited energy. The formalism in section 2.5 has been used with success in comparing experimental data in

the nanometer range from the detector setup in sections 3.3.1, 3.3.2, and 3.3.3 with Monte Carlo simulations.

It seems that no corresponding formalism has been used for variance measurements. In principle, it should be possible to connect expressions such as equation 2.20 to the data from an experiment using the variance method with a known set of impact parameters, see e.g. section 4.2.1.3.

4.3.2 Simulations

While simulations, e.g based on Monte Carlo-techniques, of micro-dosimetric interactions, has not been discussed at all in this prestudy, such simulations are vital for better understanding the mechanisms of radiation interaction at the cell- and DNA scales in living tissue. Results from simulations can also serve as benchmarks for experimental micro/nanodosimetry.

Of particlular interest for the present detector-oriented work is to be able to predict how a new type of detector will behave in a specific radiation environment. For this purpose various types of computer simulations would indeed prove useful. This could include advanced Monte Carlo-based simulations of the detector volume and geometry. In fact, Monte Carlo simulations of all the detector geometries discussed above, in relevant radiation environments, would be of high interest to understand in detail the limitations of the variance method at and below the 10 nm scale. Of specific interest is the study of wall effects and effects of radiation scattering on the anode. Such simulation together with measurements could e.g. evaluate the effect of the walls and the larger anode radius in the Extradin detectors compared to the Columbia detectors, see section 4.2.1.1. Similarly, simulations could be used to predict how the detector *size* for both spherical and parallel-plate detectors affect the relative signal uncertainty (related to V_b and Q_b of section 3.1.2) originating from various wall/anode effects. Simulations of the miniature ionization chambers, surrounded of e.g. a water phantom, in a proton beam geometry is also of high interest.

In experimental nuclear- and particle physics it has become more common in recent years to make a type of *coupled simulations* that include both the physical process of the interaction between radiation particles and matter in specific volume and the detection process itself. A combined simulation of the radiation physics (particle track structures, ionization distributions) and detector response (electron transport, noise generation, etc) could e.g. be valuable for investigating untested novel detector designs for nanodosimetry. This type of simulation can generate an output in principle corresponding to the experimental data (e.g. time-dependent integrated charge values). The simulated data can be analysed with the standard procedures, and can be compared with (or used to approximately predict) the experimental data. As one example, this would allow for predictions of the co-variance term C_r for certain measurements with two detectors. There could be a value in developing such a code, coupled to Monte Carlo-simulations, when evaluating new detector designs operating at simulated sizes of nanometer scale.

4.4 Summary

The objectives specifically mentioned in the original prestudy proposal [43] are listed here and commented in the context of this report. While the overview of quantities and methods given in chapter 2 was not specified in the project proposal it gives some rele-

vant background for the discussion in chapter 3, specifically regarding limiting factors at the nanometer scale.

- A brief summary of detectors and micro-dosimetric measurement techniques at SSM was given in chapter 4.
- An overview of currently existing detector methods potentially suitable for nanodosimetry is given in chapter 3, with focus on gas detectors at low pressure and including a presentation of a few novel techniques aiming at track dosimetry at the nano-metre scale.
- A need for detailed simulations of relevant detector designs is identified in chapter 4. Both Monte Carlo-simulations of the physical radiation interaction and simulations of the detector response process, e.g. charge collection are of interest.
- Relevant detector types and measurements for future work at SSM was discussed in chapter 4 and some conclusions are summarized here:
  - Today's generation of semiconductor microdosimeters, such as silicon-on-insulator or $\Delta E - E$ designs are not suitable for measurements in the 10 nm region.
  - Spherical, cylindrical, and parallel plate gas-filled detectors at gas pressures low enough have the potential for simulating nanometer size sites using the variance technique for both low- and high LET radiation fields. A need to experimentally test some aspects of the detector design is identified.
  - A possible way to firmly establishing the variance measurement technique at simulated sizes even below 10 nm simulated size would be to build *larger* prototype detectors than is used at SSM today; gas volume diameters of 10-30 cm could be investigated. Large vacuum chambers at well-controlled pressure would be needed for this.
  - A better understanding on how background/noise currents are generated is necessary, especially for smaller devices. The dependence on background currents of anode wire size and geometry at gas pressures corresponding to the nanometer scale could be investigated both with simulations and measurements, e.g. comparing results for different anode diameters.
  - The potential of using a multi-channel-plate (or GEM) and pixelized readout chips as a charge-collecting device in a parallel-plate-geometry gas detector is of high interest, aiming at ionization track dosimetry, but would require considerable development work. One challenge is how to operate the devices in the pressure region relevant for nanodosimetry. This design could be investigated as a separate future project, perhaps within the framework of a MSc thesis or as part of a PhD project.
  - The behaviour of secondary electrons escaping from the walls of ionization chambers has been previously studied in some detail, see e.g. Ref. [34]. The potential of utilizing this effect for nanodosimetry in the 10 nm range could be further investigated. Implementing detectors using this principle would involve considerable development work, and a separate study (e.g. a MSc project) could explore the potential based on Monte Carlo simulations. The

output from such simulations overlap with the interest of understanding secondary electron contributions in standard ionization chambers, as discussed above in chapter 4.

- Based on the above, a possible strategy for further experimental work at SSM would be the following:
  - Re-establishing variance measurements of $\bar{y}_D$ in the 10 nm range using two types of existent different gas detectors (The Extradin detectors and the wall-less Columbia detector) in the ^{60}Co field at SSM. Of particular interest is using the Columbia detector in different modes, i.e. using not only spherical volume but also the inner cylindrical volume enclosed by the helix as the sensitive gas volume, see section 4.2.1.1.
  - Compare existing low-noise electrometer hardware (Electrometers A&B) with modern commercial electrometers.
  - Test miniature ionization chambers in the ^{60}Co field.
  - Build and test (and simulate) various detector geometries: a larger wall-less ionization chamber based on the Columbia design and parallel-plate ionization chambers of different sizes and with different detector/field geometries, see above. Investments in new vacuum systems / pressure monitoring might be needed for these measurements.
  - Simulate, using a simple software model, the influence for different detectors and electrometer setups of secondary electrons and electronic noise. The objective would be to better understand the limiting factors for the variance method in the nanometer region.
  - Perform measurements in proton beams (e.g. at *Skandionkliniken* in Uppsala), with miniature ionization chambers and optionally with a small parallel-plate design.
- As mentioned in section 4.3.1, it should be of interest to investigate how the ionization cluster probability formalism, see section 2.5, would relate to data extracted from measurements using the variance method. Output from Monte-Carlo simulations should be useful also for this purpose.

Acknowledgement

The author thanks the staff of the Swedish secondary dosimetry laboratory at SSM for their kind assistance and for answering a large number of questions about micro/nano-dosimetric measurements. Special thanks goes to Jan Lillhök for many fruitful discussions, to Göran Samuelsson for explaining (at least part of) the mysteries of low-noise electrometer design, and to Christian Iacobaeus for discussions on novel detector designs aiming at future track dosimetry measurements.

Bibliography

[1] D.E. Lea. *Actions of Radiation on Living Cells*. Cambridge Univ. Press, 1955.

[2] H.H. Rossi. Specification of radiation quality. *Radiation Research*, 10:522, 1959.

[3] H.H. Rossi. Spatial distribution of energy deposition by ionizing radiation. *Radiation Research Suppl.*, 2:290, 1960.

[4] H.H. Rossi. *Radiation Dosimetry*, chapter Microscopic Energy Distribution in irradiaded matter. Academic Press, 1968.

[5] H.H. Rossi. The role of microdosimetry in radiobiology and radiation protection. In *Proc. of the 3:rd Symposium on Microdosimetry*, 1972.

[6] J. Lillhök. *The microdosimetric variance-covariance method used for beam quality characterization in radiation protection and radiation therapy*. PhD thesis, Stockholm University, 2007.

[7] D.J. Brenner and J.F. Ward. Constraints on energy deposition and target size of multiple damaged sites associated with DNA double-strand breaks. *Rad.Bio.*, 61:737–748, 1992.

[8] Microdosimetry. Technical Report 36, ICRU, 1983.

[9] H.H Rossi and M. Zaider. *Microdosimetry and Its Applications*. Springer, 1996.

[10] A.M. Kellerer. *Dosimetry of Ionizing Radiation*, volume 1, chapter Fundamentals of Microdosimetry, pages 77–162. Academic Press, 1985.

[11] L. Lindborg and H. Nikjoo. Microdosimetry and radiation quality determinations in radiation protection and radiation theraphy. *Rad.Pro.Dos.*, 143:402–408, 2011.

[12] L. Lindborg et al. Lineal energy and radiation quality in radiation theraphy: Model calculations and comparison with experiment. *Phys. Med.Biol.*, 58:3089–3105, 2013.

[13] L. Lindborg et al. Nanodosimetry and RBE values in radiotheraphy. *Rad.Pro.Dos.*, 166:339–342, 2015.

[14] L.G. Bengtsson. Assessment of dose equivalent from fluctuation of energy deposition. In *Proc. of the Second Symposium on Microdosimetry*, volume EUR 4452, pages 375–395. Euroatom, 1970.

[15] L.G. Bengtsson and L. Lindborg. Comparison of pulse height analysis and variance measurement of the determination of dose mean specific energy. In *Proc. of the Forth Symposium on Microdosimetry*, volume EUR 5122, pages 823–841. Euroatom, 1974.

[16] A.M. Kellerer and H.H. Rossi. On the determination of microdosimetric parameters in time-varying fields: the variation-covariation method. *Radiation Research*, 97:237–245, 1984.

[17] H.I. Amols et al. On possible limitations of experimental nanodosimetry. *Rad.Pro.Dos.*, 31:125–128, 1990.

[18] L. De Nardo et al. Ionization-cluster distributions of alpha-particles in nanometric volumes of propane: measurement and calculation. *Rad. Env. Bioph.*, 41:235–256, 2002.

[19] B. Grosswendt. Recent advances of nanodosimetry. *Rad.Pro.Dos.*, 110:789–799, 2004.

[20] B. Grosswendt, S. Pszona, and A. Bantsar. New descriptors of radiation quality based on nanodosimetry, a first approach. *Rad.Pro.Dos.*, 126:432–444, 2007.

[21] V. Conte et al. First track-structure measurements of 20 MeV protons with the STARTRACK apparatus. *Rad.Meas.*, 45:1213–1216, 2010.

[22] B. Grosswendt. Formation of ionization clusters in nanometric structures of propane-based tissue-equivalent gas or liquid water by electrons and α-particles. *Rad.Env.Biophys.*, 41:103–112, 2002.

[23] H. Palmans et al. Future development of biologically relevant dosimetry. *Br.J.Radiol.*, 88, 2014.

[24] J. E. Grindborg, G. Samuelsson, and L. Lindborg. Variance-covariance measurements in photon beams for simulated nanometre objects. *Rad.Prot.Dos.*, 61:193–198, 1995.

[25] E.A. Bigildeev and A.V. Lappa. Determination of energy deposited in nanometre sites from ionisation data. *Rad.Prot.Dos.*, 52:73–76, 1994.

[26] W.A. Glass and W.A. Gross. Wall-less detectors in microdosimetry. In *Topics in Radiation Dosimetry*, page 221. Academic Press, 1972.

[27] L. Lindborg et al. Microdosimetric measurements and the variance-covariance method. *Rad.Env.Bioph.*, 28:251–263, 1989.

[28] B. Forsberg and L. Lindborg. Experimental limitations in microdosimetry measurements using the variance technique. *Rad.Env.Bio.*, 19:125–135, 1981.

[29] M. Orlic et al. Microdosimetric counters based on semiconductor detectors. *Rad.Pro.Dos.*, 29:21–22, 1989.

[30] A.B. Rosenfeld et al. A new silicon detector for microdosimetry applications in proton therapy. *IEEE Trans Nucl. Sci.*, 47:1386, 2000.

[31] A.B. Rosenfeld. Novel detectors for silicon based microdosimetry, their concepts and applications. *NIM A*, 809:156–170, 2016.

[32] K.R. Ennow. Measurements of the variance of energy deposition by means of exo-electron emitting materials. In *Proc. of the Fourth Symposium on Microdosimetry*, volume EUR 5122, page 925, 1974.

[33] T.E. Burlin. The characteristics of secondary electron emission and some potential applications to microdosimetry. In *Proc. of the Fourth Symposium on Microdosimetry*, volume EUR 5122, page 35, 1974.

[34] B.J. Forsberg and T.E. Burlin. Microdosimetry. I. use of secondary electron emission. *Acta Rad. Onc.*, 19:115, 1980.

[35] G. Garty et al. The performance of a novel ion-counting nanodosimeter. *NIM A*, 492:212, 2002.

[36] S. Pszona and R. Gajewski. An approach to experimental microdosimetry at the nanometre scale. *Rad.Prot.Dos.*, 52:427, 1994.

[37] A. Bantsar et al. Single-track nanodosimetry of low energy electrons. *NIM A*, 599:270, 2009.

[38] L. De Nardo et al. A detector for track-nanodosimetry. *NIM A*, 484:312–326, 2002.

[39] Riksmätplatsen. www.stralsakerhetsmyndigheten.se/Yrkesverksam/Riksmatplatsen/, 2016.

[40] J. Lillhök. Private communication, 2016.

[41] Medipix webpage. http://medipix.web.cern.ch/medipix/, 2016.

[42] Photonis webpage. https://www.photonis.com/uploads/literature/mcp/Handling-Storage-Instructions-EN.pdf, 2016.

[43] Projektansökan till SSM: Detektorer för variansmätningar i nanometerområdet - förstudie. Project proposal, submitted to SSM, 2015.

2018:13

The Swedish Radiation Safety Authority has a comprehensive responsibility to ensure that society is safe from the effects of radiation. The Authority works to achieve radiation safety in a number of areas: nuclear power, medical care as well as commercial products and services. The Authority also works to achieve protection from natural radiation and to increase the level of radiation safety internationally.

The Swedish Radiation Safety Authority works proactively and preventively to protect people and the environment from the harmful effects of radiation, now and in the future. The Authority issues regulations and supervises compliance, while also supporting research, providing training and information, and issuing advice. Often, activities involving radiation require licences issued by the Authority. The Swedish Radiation Safety Authority maintains emergency preparedness around the clock with the aim of limiting the aftermath of radiation accidents and the unintentional spreading of radioactive substances. The Authority participates in international co-operation in order to promote radiation safety and finances projects aiming to raise the level of radiation safety in certain Eastern European countries.

The Authority reports to the Ministry of the Environment and has around 300 employees with competencies in the fields of engineering, natural and behavioural sciences, law, economics and communications. We have received quality, environmental and working environment certification.

Strålsäkerhetsmyndigheten
Swedish Radiation Safety Authority

SE-171 16 Stockholm
Solna strandväg 96

Tel: +46 8 799 40 00
Fax: +46 8 799 40 10

E-mail: registrator@ssm.se
Web: stralsakerhetsmyndigheten.se

Ale Tryckteam AB, Bohus, 2018